

# High-Speed Silicon-Organic Hybrid (SOH) Modulators with 230 pm/V Electro-Optic Coefficient Using Advanced Materials

R. Palmer<sup>1</sup>, S. Koeber<sup>1</sup>, M. Woessner<sup>1</sup>, D. L. Elder<sup>2</sup>, W. Heni<sup>1</sup>, D. Korn<sup>1</sup>, H. Yu<sup>3,4</sup>, M. Lauer<sup>1</sup>,  
W. Bogaerts<sup>3</sup>, L. R. Dalton<sup>2</sup>, W. Freude<sup>1</sup>, J. Leuthold<sup>1,5</sup>, C. Koos<sup>1</sup>

<sup>1</sup>Karlsruhe Institute of Technology (KIT), Institutes IPQ and IMT, Engesserstr. 5, 76131 Karlsruhe, Germany

<sup>2</sup>University of Washington, Department of Chemistry, Seattle, WA 98195-1700, United States

<sup>3</sup>Ghent University – IMEC, Photonics Research Group, Department of Information Technology, Gent, Belgium

<sup>4</sup>now with: Zhejiang University, Department of Information Science and Electronic Engineering, Hangzhou 310027, China

<sup>5</sup>Electromagnetic Fields Laboratory, Swiss Federal Institute of Technology (ETH), Zurich, Switzerland

[robert.palmer@kit.edu](mailto:robert.palmer@kit.edu), [christian.koos@kit.edu](mailto:christian.koos@kit.edu)

**Abstract:** We report on record-high electro-optic coefficients of up to 230 pm/V in silicon slot waveguide modulators. The modulators allow for low drive voltage at 40 Gbit/s at a device length of only 250  $\mu\text{m}$ .

**OCIS codes:** (230.4110) Modulators; (060.4080) Modulation

## 1. Introduction

Silicon-organic hybrid (SOH) devices combine the advantages of strongly guiding silicon photonic waveguides with the wealth of optical properties accessible by molecular engineering of organic materials. In particular, efficient phase modulation can be achieved in SOH devices by using organic cladding materials with pronounced electro-optic (EO) activity. So far, the most commonly used EO materials for SOH integration were polymers doped by small percentages of EO chromophore molecules [1, 2]. However, while these guest-host materials have shown EO coefficients as high as 155 pm/V in bulk material [1], values measured in SOH devices were so far limited to approximately 60 pm/V [2]. Small in-device EO coefficients remained an unsolved issue, preventing the use of the full potential of SOH integration. These limitations have recently been overcome by using a novel class of so-called monolithic EO materials [3], which do not require a polymer matrix to prevent dipole-dipole interaction of chromophores that would lead to vanishing macroscopic EO activity. Such a monolithic material (DLD164) has been applied to an SOH Mach-Zehnder modulator (MZM), resulting in a strong increase of the in-device EO-coefficient to 180 pm/V, allowing for switching energies as low as 1.6 fJ/bit. [4]

In this work we demonstrate that even higher in-device EO coefficients of up to 230 pm/V can be achieved by a mixture of traditional EO chromophores and multi-chromophore dendritic molecules (dendron). The extraordinarily high EO coefficient results in a voltage-length product  $V_{\pi}L$  as small as 0.5 Vmm measured at DC. This enables 250  $\mu\text{m}$  long SOH Pockels-effect modulators driven by source voltages as small as 2.1 V<sub>pp</sub> at data rates of up to 40 Gbit/s, where an ER of 9 dB is achieved. We benchmark the results by comparison with a guest-host EO material and with two different monolithic EO materials.

## 2. Silicon-Organic Hybrid Modulator

The MZM used in this work is illustrated in Fig. 1(a). It consists of two SOH phase-modulators, Fig. 1(b), that are driven in push-pull configuration by a single coplanar transmission line (GSG). The copper electrodes of the transmission line are connected to the phase-modulators by 900 nm high tungsten vias. A schematic of a SOH phase modulator along with the electric field of the fundamental quasi-TE mode is depicted in Fig. 1(b). The phase modulator consists of a slot waveguide that is electrically connected to an RF transmission line by 60 nm thick doped (As,  $7 \times 10^{17} \text{cm}^{-3}$ ) silicon strips. The voltage applied to the transmission line drops across the narrow slot, resulting in a high electric field. At the same time, the optical mode is strongly confined to the slot region, resulting in a high overlap with the modulating field. The waveguide is covered and the slot is filled with an electro-optic organic material that is deposited by spin-coating. Directly after the deposition, the organic material does not feature any macroscopic EO effect due to the random orientation of the chromophores. A poling procedure is necessary to induce a macroscopic EO activity. This is accomplished by heating the sample to the glass-transition temperature  $T_g$  of the organic material while applying an electric DC field to align the dipolar molecules [5]. While holding the poling voltage, the chip is cooled back to room temperature, thereby conserving the acentric order of the chromophores. The devices are fabricated by deep-UV lithography on a 220 nm SOI wafer with 2  $\mu\text{m}$  buried oxide. The measured slot width is 160 nm and the rail width is 210 nm. The fiber-to-fiber loss is 16.5 dB, dominated by fiber-to-chip coupling losses of the non-optimized grating couplers. The on-chip loss is approximately 6 dB for maximum transmission of the modulator. Two SOH MZM of different lengths were investigated: Fig. 1(c) depicts the measured bandwidths of a 1 mm-long modulator terminated with 50  $\Omega$ , and of a 250  $\mu\text{m}$ -long non-terminated modulator. The 6 dB electrical-optical-electrical (EOE) bandwidths are 18 GHz and 22 GHz, respectively. Applying a gate voltage between the substrate and the transmission line allows to further boost the bandwidth as reported in [6].

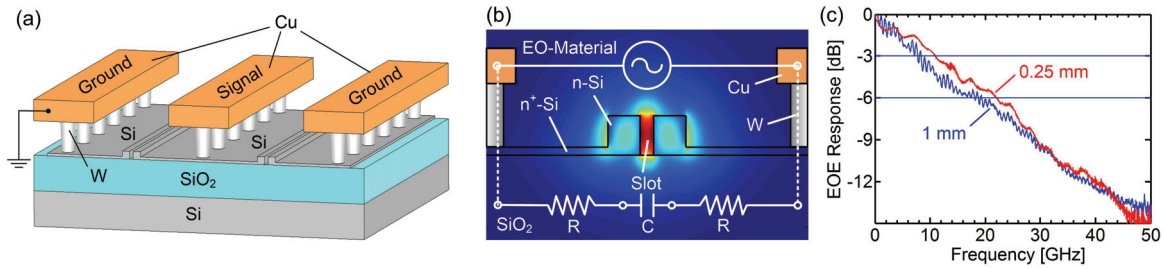


Fig. 1 (a) Schematic of the MZM. The device consists of two phase modulators driven in push-pull operation by a single coplanar transmission line (ground-signal-ground). (b) Schematic and simulated optical mode of one arm of the MZM. The two rails of the silicon slot waveguide are electrically connected to metal electrodes by 60 nm high n-doped (As,  $7 \times 10^{17} \text{ cm}^{-3}$ ) silicon slabs. The modulation voltage drops across the narrow slot resulting in a high modulation field that has a strong overlap with the optical mode. The silicon slot is filled with an electro-optic organic material. (c) Measured electrical-optical-electrical (EOE) response of a 1 mm long terminated MZM and of a 250  $\mu\text{m}$  long non-terminated MZM, both covered with the organic material mixture YLD124/PSLD41. The 6-dB EOE bandwidths are 18 GHz and 22 GHz, respectively.

### 3. Poling Results of the Investigated Electro-Optic Organic Materials

The materials investigated in this work are the monolithic chromophore DLD164 [4], the multi-chromophore dendritic molecule PSLD41 [7], the guest-host material YLD124 (25 wt.%) in PMMA [1], and a mixture of YLD124 and PSLD41 (25:75 wt.%). The respective chemical structures are depicted in Fig. 2. DLD164, Fig. 2(b), and PSLD41, Fig. 2(d), are structurally engineered molecules optimized for enhanced poling efficiency. For DLD164, pendant coumarin-containing sidegroups mitigate dipole-dipole interaction and are used to reduce the rotational degrees of freedom of the chromophores from three to two. This improves the degree of chromophore alignment for a given poling field by roughly a factor of two [8]. The dendritic chromophore PSLD41 uses a different approach. Here, perfluoraryl-containing side-groups are used to effectively reduce the dipole-dipole interaction of neighboring molecules. The dendron chromophore consists of a central connecting motif to which three EO substructures are attached, see Fig. 2(d). This results in a spherical shape of the molecule and improved poling efficiency [3]. The investigated materials are applied to nominally identical chips by spin-coating from an 8% solution dissolved in 1,1,2-trichloroethane. After deposition, the materials are poled for a later push-pull operation of the MZM by applying a poling voltage between the ground electrodes of the modulator [5]. After poling, the  $\pi$ -voltage  $V_\pi$  of the modulator is measured at DC so that the EO coefficient can be derived. Fig. 2(a) depicts the resulting EO coefficients as a function of the applied poling field for the various materials. The first investigated material is the guest-host system YLD124/PMMA. Similar to previously reported results in other guest-host systems [2, 5, 6] we reach only small  $r_{33}$ -values ( $\leq 29 \text{ pm/V}$ ) and a low poling efficiency  $r_{33}/E_{\text{poling}}$  of only  $0.23 \text{ nm}^2/\text{V}^2$  measured for small poling fields. This is far below the value achieved in the corresponding bulk material [1]. Next, we study the monolithic chromophore DLD164. We find a much higher poling efficiency ( $1.17 \text{ nm}^2/\text{V}^2$ ) and a large  $r_{33}$  of up to 190 pm/V. Finally we perform poling experiments with a sample coated with pure PSLD41 and with a sample coated with the binary chromophore organic glass YLD124/PSLD41. For PSLD41, we find a remarkable in-device  $r_{33}$  of 97 pm/V (poling efficiency  $0.31 \text{ nm}^2/\text{V}^2$ ) while the composition YLD124/PSLD41 results in even higher values of up to 230 pm/V (poling efficiency  $0.92 \text{ nm}^2/\text{V}^2$ ). This finding is in good agreement with results obtained in bulk material, where the binary chromophore system YLD124/PSLD41 was also found to have an  $r_{33}$  coefficient that exceeds even the sum of the  $r_{33}$  coefficients of its constituents [7]. This is the highest reported EO coefficient in an SOH device, and is even

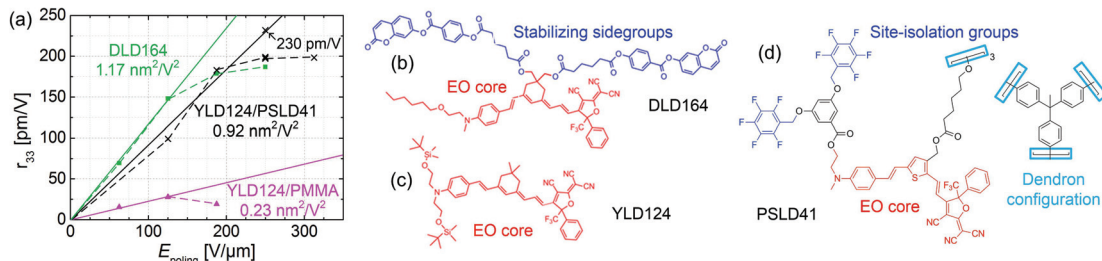


Fig. 2 (a) Measured poling efficiencies  $r_{33}/E_{\text{poling}}$  for three different organic cladding materials: The monolithic chromophore DLD164, PMMA doped with 25%wt. YLD124 (guest-host system), and the dendritic chromophore PSLD41 doped by 25%wt. YLD124 (binary chromophore organic glass). The materials DLD164 and PSLD41 consist of structurally engineered chromophores that enable high chromophore densities and a high degree of chromophore orientation during poling. We find extraordinarily high in-device electro-optic coefficients for DLD164 (190 pm/V) and YLD124/PSLD41 (230 pm/V). (b-d) The chemical structures of the individual chromophores are depicted. The EO-cores of the chromophores are drawn in red. Sidegroups, that lead to matrix stabilization and enhancement of molecular orientation are marked in blue. PSLD41 is a dendritic configuration that combines three EO substructures, marked in light blue in (d).

Table 1 – Summary of measured EO coefficients. Comparison between in-device values and values achieved in parallel-plate poled bulk reference samples.

Material	$n$	$r_{33}$ in-device [pm/V]	$r_{33}$ bulk [pm/V]	$n^3 r_{33}$ in-device [pm/V]	$V_{\pi}L$ [Vmm]	$T_g$ [°C]
YLD124(25wt. %)/PMMA	1.7	29	155 [1]	142	4.10	105
DLD164	1.83	190	137	1164	0.48	66
PSLD41	1.72	97	90 [7]	494	1.23	103
YLD124(25wt. %)/PSLD41	1.73	230	285 [7]	1130	0.52	97

higher than the previously reported record value of a fully organic MZM, where 137 pm/V were measured [9]. Table 1 summarizes the results of the poling experiments of the four investigated materials. We see that in contrast to guest-host systems like YLD124 in PMMA, where in-device EO coefficients are usually much smaller than reference values of bulk materials, structurally engineered chromophores like DLD164 or PSLD41 allow for values close to or even higher than the bulk-material reference. This is partially due to the fact that the materials exhibit higher stability with respect to dielectric breakdown in SOH slot waveguides than in bulk references. We attribute this to thin-film effects and low defect densities in the slot region. Note that the in-device  $n^3 r_{33}$  figures of merit of the reported organic materials exceed 1100 pm/V and are clearly superior to those of conventional EO materials such as GaAs ( $n^3 r_{33} \approx 60$  pm/V) and LiNbO<sub>3</sub> ( $n^3 r_{33} \approx 400$  pm/V).

#### 4. Demonstration of 40 Gbit/s OOK

Finally, we perform high-speed modulation experiments based on 250  $\mu\text{m}$ -long non-terminated MZM modulators coated with the mixture YLD124/PSLD41. Light from a tunable laser source at 1540 nm is coupled to the modulator, which is biased to its quadrature point. The device is connected to a pattern generator adjusted for a peak-to-peak voltage of 2.1 V<sub>pp</sub> if terminated with 50  $\Omega$ . Reflections of the RF wave at the end of the non-terminated device result in nearly a doubling of the in-device drive voltage to roughly 4.2 V<sub>pp</sub>. The modulated light is amplified using an EDFA and received using a digital communications analyzer along with a bit error ratio (BER) tester. Fig. 3 shows recorded eye diagrams for data rates from 25 Gbit/s to 40 Gbit/s. We observe excellent signal quality and extinction ratios (ER) exceeding 10 dB up to a data rate of 35 Gbit/s. At 40 Gbit/s we measure a low BER of  $2 \times 10^{-6}$  and an ER of 9 dB. The modulator has a measured capacitance of 95 fF resulting in an energy consumption of 420 fJ/bit [4]. It is possible to reduce the energy consumption to a few fJ/bit by increasing the modulator length to 1 mm as reported in [4]. Note that, in contrast to earlier demonstrations of 40 Gbit/s SOH modulators [4, 6], we did not use a gate voltage to improve the silicon conductivity [6]. Still, a small voltage-length product of 1 Vmm is found for operation at 40 Gbit/s, one order of magnitude below typical values reported for reverse-biased pn-modulators [10].

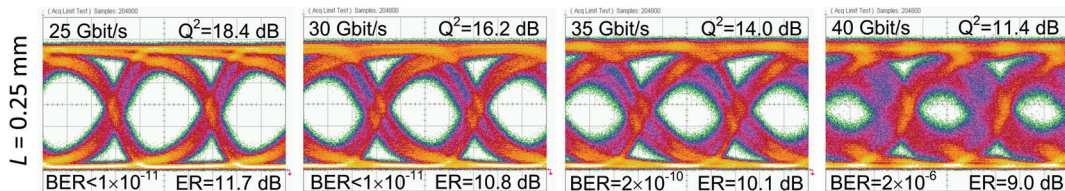


Fig. 3 NRZ OOK eye diagrams at 25 Gbit/s, 30 Gbit/s, 35 Gbit/s, and 40 Gbit/s obtained from a 250  $\mu\text{m}$ -long MZM without termination. Measured  $Q^2$ -factors, extinction ratios (ER) and bit error ratios (BER) are denoted in the figure. Drive voltage across the slot is 4.2 V<sub>pp</sub>. The ER exceeds 10 dB up to 35 Gbit/s. At 40 Gbit/s we measure a BER of  $2 \times 10^{-6}$ . PRBS length  $2^{31}-1$ . No gate voltage has been used.

#### 5. Conclusion

We demonstrate that EO coefficients as high as 230 pm/V can be achieved by hybridizing silicon slot waveguides with structurally engineered electro-optic organic materials. This allows for small voltage-length products of 0.5 Vmm, enabling non-resonant 250  $\mu\text{m}$ -long devices operating at 40 Gbit/s.

We acknowledge support by the European Research Council (ERC Starting Grant ‘EnTeraPIC’, number 280145), the EU-FP7 projects SOFI, OTONES, and PHOXTR0T, the Alfried Krupp von Bohlen und Halbach Foundation, the Karlsruhe School of Optics and Photonics (KSOP), the DFG Center for Functional Nanostructures (CFN), the Karlsruhe International Research School for Teratronics (HIRST), and the Karlsruhe Nano-Micro Facility (KNMF). We acknowledge financial support of the National Science Foundation (DMR-0905686, DMR-0120967) and the Air Force Office of Scientific Research (FA9550-09-1-0682).

#### 6. References

- [1] P. A. Sullivan et al., *Accounts Chem. Res.* vol. 43(1), 2010.
- [2] X. Wang et al., *Opt. Lett.*, vol. 36(6), 2011.
- [3] L. R. Dalton et al., *Chem. Rev.*, vol. 110(1), 2010.
- [4] R. Palmer et al., *ECOC 2013*, paper We.3.B.3.
- [5] R. Palmer et al., *PTL*, vol. 25(13), 2013.
- [6] L. Alloatti et al., *Opt. Express*, vol. 19(2), 2011.
- [7] Y. V. Pereverzev et al., *J. Phys. Chem. C*, vol. 112, 2008.
- [8] L. R. Dalton et al., *Opt. Mater.*, vol. 32(6), 2010.
- [9] Y. Enami et al., *Nature Photonics* 1, pp. 180-185, 2007.
- [10] G. T. Reed et al., *Nature Photon.*, vol. 4, pp. 518–526, 2010.